Int. J. Heat Mass Transfer. Vol. 30, No. 7, pp. 1511–1523, 1987
Printed in Great Britain

0017–9310/87 $3.00 + 0.00
Pergamon Journals Ltd.

Laminar three-dimensional mixed convection about a rotating sphere in a stream

GEORGES LE PALEC
Groupe de Recherche en Génie Thermique, Institut Universitaire de Technologie, Rue Engel Gros, 90016 Belfort Cédex, France

and

MICHEL DAGUENET
Laboratoire de Thermodynamique et Energétique, Université de Perpignan, Avenue de Villeneuve, 66025 Perpignan Cédex, France

(*Received* 13 *May* 1986 *and in final form* 5 *February* 1987)

Abstract—The power series of several variables has been applied to study the laminar mixed convection about an isothermal rotating sphere in a stream of arbitrary direction with respect to the axis of rotation, so that the velocity profile is three-dimensional. The boundary layer equations are numerically solved and results are presented for values of the rotation parameter and the buoyancy parameter ranging from 0 to 10. For some particular cases, qualitative and quantitative comparisons with previous works reported in the literature agree with each other. Moreover, the agreement between the theoretical results and the experimental data is satisfactory.

1. INTRODUCTION

BECAUSE of their applications in many industrial processes as in chemical or electrochemical engineering, the heat and mass transfer to rotating bodies of revolution in a stream has been the subject of several investigations. Lee *et al.* [1] studied the laminar boundary layer over a rotating sphere in forced flow when the angle β_i between the stream and the axis of rotation is equal to zero. Furuta *et al.* [2] measured the local and average mass transfer for the same problem and experimental results were in good agreement with the theoretical ones. These authors also carried out experiments for the cases $\beta_i = 45°$ and 90° [3], but there is no theoretical work on this subject. On the other hand, the combined forced and free convection around a stationary sphere has been investigated by Chen and Mucoglu [4], while free convection around rotating bodies of revolution was considered by Bachrun [5] and Suwono [6]. However, in these two last works, no axial stream occurs.

More recently, the present authors [7] proposed a theoretical analysis of the effects of buoyancy force on a laminar boundary layer over a rotating sphere which is situated in an axial stream. In this connection, a later similar study of Rajasekaran and Palekar [8] should be noted. In the present work, power series of several dimensionless variables are used in order to study the three-dimensional effects of the flow when the angle β_i is not equal to zero. The mathematical model leads to the determination of the local and average heat transfer rates and the components of the local friction factor. Results are first given for gases with a Prandtl number of 1. Finally, experimental results which were obtained by an electrochemical method are compared with the theoretical ones for a Schmidt number of 2730.

2. THEORETICAL ANALYSIS

Consider a sphere of radius L which is situated in a uniform flow with oncoming free stream velocity U_∞ and temperature T_∞, as shown in Fig. 1. The convective forced flow moves upward, while gravity g_a acts in the opposite direction. The axis of rotation is inclined with an angle β_i from the direction of the stream. The surface temperature of the sphere T_w is constant and consideration is given to steady, laminar, non-dissipative and incompressible boundary layer flow. All physical properties of the fluid are assumed constant, except the density changes which produce buoyancy forces.

We choose coordinates x, y and θ with x representing the distance measured along a meridian curve from the forward stagnation point, y measuring the normal distance from the surface of the sphere and θ the azimuthal direction. θ is positive when the spin of the sphere aids the forced flow and is negative in the opposite case. Thus, the variations of θ are included in the range $-\pi < \theta < \pi$. Let V_x, V_y and V_θ be the components of velocity in the x-, y- and θ-directions, respectively. The conservation equations of the laminar boundary layer can be written as [9]

$$\frac{\partial V_x}{\partial x} + \frac{\partial V_y}{\partial y} + \frac{1}{r}\frac{\partial V_\theta}{\partial \theta} + \frac{V_x}{r}\frac{\mathrm{d}r}{\mathrm{d}x} = 0 \qquad (1)$$

NOMENCLATURE

B rotation parameter, equation (9)
C_ε ε component of the local friction factor, equation (29)
C_θ θ component of the local friction factor, equation (29)
$f(\varepsilon, \eta, \phi)$ reduced stream function, equation (13)
$g(\varepsilon, \eta, \phi)$ reduced stream function, equation (13)
g_a gravitational acceleration [m s^{-2}]
Gr Grashof number
h heat transfer coefficient, equation (30) [W m^{-2} K^{-1}]
L radius of the sphere [m]
Nu local Nusselt number, equation (29)
$\overline{Nu}$ average Nusselt number, equation (33)
Pr Prandtl number
r radial distance from axis (Fig. 1) [m]
Re_∞ Reynolds number, equation (11)
S area of the sphere [m^2]
$\overline{Sh}$ average Sherwood number
T fluid temperature [K]
T_w wall temperature [K]
T_∞ free stream temperature [K]
U local free velocity [m s^{-1}]
U_∞ undisturbed oncoming free stream velocity [m s^{-1}]
V_x component of the velocity in the x-direction [m s^{-1}]
V_y component of the velocity in the y-direction [m s^{-1}]
V_θ component of the velocity in the θ-direction [m s^{-1}]
x, y coordinates shown in Fig. 1 [m].

Greek symbols
α thermal diffusivity [m^2 s^{-1}]
β_t coefficient of thermal expansion [K^{-1}]
β_i angle between the direction of forced flow and the axis of rotation (Fig. 1) [rad or deg]
ε, η, ϕ system of dimensionless coordinates, equation (12)
λ thermal conductivity of the fluid [W m^{-1} K^{-1}]
θ radial coordinate shown in Fig. 1 [rad]
θ_T dimensionless temperature, equation (13)
μ dynamic viscosity of the fluid [N s m^{-2}]
ν kinematic viscosity of the fluid [m^2 s^{-1}]
ρ density of the fluid [kg m^{-3}]
τ_x component of the wall shear stress in the x-direction [N m^{-2}]
τ_θ component of the wall shear stress in the θ-direction [N m^{-2}]
ψ, ϕ stream functions which depend on x, y and θ [m^2 s^{-1}]
ω spin velocity of the sphere [rad s^{-1}]
Ω buoyancy force parameter, equation (10).

$$V_x\frac{\partial V_x}{\partial x}+V_y\frac{\partial V_x}{\partial y}+\frac{V_\theta}{r}\frac{\partial V_x}{\partial \theta}-\frac{V_\theta^2}{r}\frac{\mathrm{d}r}{\mathrm{d}x}=\nu\frac{\partial^2 V_x}{\partial y^2}+U\frac{\mathrm{d}U}{\mathrm{d}x}+(T-T_\infty)g_a\beta_t\sin\frac{x}{L} \quad (2)$$

$$V_x\frac{\partial V_\theta}{\partial x}+V_y\frac{\partial V_\theta}{\partial y}+\frac{V_\theta}{r}\frac{\partial V_\theta}{\partial \theta}+\frac{V_xV_\theta}{r}\frac{\mathrm{d}r}{\mathrm{d}x}=\nu\frac{\partial^2 V_\theta}{\partial y^2} \quad (3)$$

$$V_x\frac{\partial T}{\partial x}+V_y\frac{\partial T}{\partial y}+\frac{V_\theta}{r}\frac{\partial T}{\partial \theta}=\alpha\frac{\partial^2 T}{\partial y^2}. \quad (4)$$

Equations (1)–(4) are subjected to the following boundary conditions [10]:

$$\left.\begin{aligned} &V_x=\omega L\sin\beta_i\sin\theta\\ &V_y=0\\ &V_\theta=\omega L\left(\cos\beta_i\sin\frac{x}{L}+\sin\beta_i\cos\frac{x}{L}\cos\theta\right)\\ &T=T_w\end{aligned}\right\}\ \text{at } y=0$$

$$\left.\begin{aligned} &V_x\to U\\ &V_\theta\to 0\\ &T\to T_\infty\end{aligned}\right\}\ \text{as } y\to\infty. \quad (5)$$

In the foregoing equations, the standard symbols are defined in the nomenclature. $r(x)$ is the radial distance which is given by

$$r=L\sin\frac{x}{L}. \quad (6)$$

The local free stream velocity $U(x)$ is expressed from the potential-flow solution

$$U=\frac{3}{2}U_\infty\sin\frac{x}{L}. \quad (7)$$

It should be noted that the pressure distribution around a stationary sphere in a free stream departs from the potential-flow solution at an angle of $x/L\simeq 30°$ for laminar flow [11]. Several authors [2, 12] have proposed solutions in which U/U_∞ is assumed to be expressed as an odd power series in x/L

$$U=U_\infty\left[A'\frac{x}{L}+B'\left(\frac{x}{L}\right)^3+C'\left(\frac{x}{L}\right)^5+D'\left(\frac{x}{L}\right)^7+\ldots\right] \quad (8)$$

where $A', B', C', D', \ldots$ are constants which are exper-

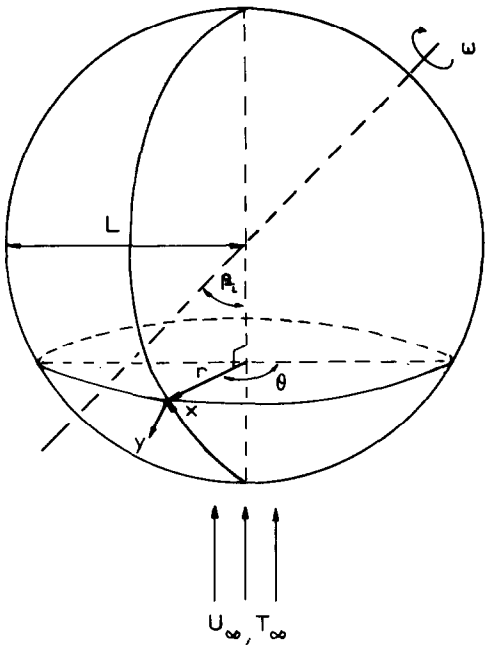

FIG. 1. The coordinate system.

imentally determined. However, if only a few terms of equation (8) are retained, the discrepancy between these solutions may be large. Thus, in order to conserve the generality of the problem, equation (7) has been chosen.

To facilitate a solution, it is convenient to introduce two dimensionless parameters:

(a) the rotation parameter

$$B = \frac{4}{9}\left(\frac{L\omega}{U_\infty}\right)^2; \tag{9}$$

(b) the buoyancy parameter

$$\Omega = \frac{Gr}{Re_\infty^2}; \tag{10}$$

wherein the Grashof number Gr and the Reynolds number Re_∞ are defined as

$$\left.\begin{aligned} Gr &= \frac{g_a \beta_t (T_w - T_\infty) L^3}{\nu^2} \\ Re_\infty &= \frac{U_\infty L}{\nu}. \end{aligned}\right\} \tag{11}$$

We now define three flow dominated cases:

(1) the buoyancy force dominated case when $\Omega > 1$ and $B < \Omega$;

(2) the rotation dominated case when $B > 1$ and $B > \Omega$;

(3) the forced flow dominated case for $B < 1$ and $\Omega < 1$.

Since our aim is to study the three-dimensional effects of the flow, it is necessary to choose moderate values of B and Ω. Thus, in the following analysis we only consider case (3); the other cases are similarly treated [9] and the appropriate transformations to do it are summarized in the Appendix.

Equations (1)–(5) are transformed from coordinates (x, y, θ) to $(\varepsilon, \eta, \varphi)$ dimensionless coordinates

$$\left.\begin{aligned} \varepsilon &= \frac{x}{L} \\ \varphi &= \theta \\ \eta &= \left(\frac{U}{L\nu\varepsilon}\right)^{1/2} y. \end{aligned}\right\} \tag{12}$$

We also introduce the reduced stream functions $f(\varepsilon, \eta, \varphi)$ and $g(\varepsilon, \eta, \varphi)$ and a dimensionless temperature $\theta_T(\varepsilon, \eta, \varphi)$

$$\left.\begin{aligned} f(\varepsilon, \eta, \varphi) &= \frac{\psi(x, y, \theta)}{(L\nu\varepsilon U)^{1/2}} \\ g(\varepsilon, \eta, \varphi) &= \frac{\phi(x, y, \theta)}{\omega r}\left(\frac{U}{L\nu\varepsilon}\right)^{1/2} \\ \theta_T(\varepsilon, \eta, \varphi) &= \frac{T(x, y, \theta) - T_\infty}{T_w - T_\infty} \end{aligned}\right\} \tag{13}$$

where the stream functions $\psi(x, y, \theta)$ and $\phi(x, y, \theta)$ satisfy the continuity equation (1) with

$$\left.\begin{aligned} V_x &= \frac{1}{r}\frac{\partial(\psi r)}{\partial y} \\ V_y &= -\frac{1}{r}\left(\frac{\partial(\psi r)}{\partial x} + \frac{\partial \phi}{\partial \theta}\right) \\ V_\theta &= \frac{\partial \phi}{\partial y}. \end{aligned}\right\} \tag{14}$$

Using equations (12) and (13) equations (14) become

$$\left.\begin{aligned} V_x &= Uf'; \quad V_\theta = \omega r g' \\ V_y &= -(L\nu\varepsilon U)^{1/2}\left[\frac{f}{R}\frac{\mathrm{d}R}{\mathrm{d}\varepsilon} + \frac{\partial f}{\partial \varepsilon} + \frac{f}{2U}\frac{\mathrm{d}U}{\mathrm{d}\varepsilon}\right. \\ &\qquad \left. + f'\frac{\partial \eta}{\partial \varepsilon} + \frac{1}{R}\frac{\partial g}{\partial \varphi}\right] \end{aligned}\right\} \tag{15}$$

the primes denoting differentiation with respect to η. Equations (6) and (7) show that $U = \frac{3}{2}U_\infty R$ with $R = r/L = \sin(x/L)$. With the introduction of equations (15), equations (1)–(5) can be transformed into

the following system of coupled equations:

$$\left.\begin{aligned} f''' + \left(\frac{1}{2} + \frac{3}{2}\frac{\varepsilon}{R}\frac{\mathrm{d}R}{\mathrm{d}\varepsilon}\right) ff'' + \frac{\varepsilon}{R}\frac{\mathrm{d}R}{\mathrm{d}\varepsilon}(1 - f'^2 + Bg'^2) + \frac{4}{9}\Omega\frac{\varepsilon \sin\varepsilon}{R^2}\theta_T \\ = \varepsilon\left[f'\frac{\partial f'}{\partial\varepsilon} - f''\frac{\partial f}{\partial\varepsilon} + \frac{B}{R}\left(g'\frac{\partial f'}{\partial\varphi} - f''\frac{\partial g}{\partial\varphi}\right)\right] \\ g''' + \left(\frac{1}{2} + \frac{3}{2}\frac{\varepsilon}{R}\frac{\mathrm{d}R}{\mathrm{d}\varepsilon}\right) g''f - \frac{2\varepsilon}{R}\frac{\mathrm{d}R}{\mathrm{d}\varepsilon} f'g' = \varepsilon\left[f'\frac{\partial g'}{\partial\varepsilon} - g''\frac{\partial f}{\partial\varepsilon} + \frac{B}{R}\left(g'\frac{\partial g'}{\partial\varphi} - g''\frac{\partial g}{\partial\varphi}\right)\right] \\ Pr^{-1}\theta_T'' + \left(\frac{1}{2} + \frac{3}{2}\frac{\varepsilon}{R}\frac{\mathrm{d}R}{\mathrm{d}\varepsilon}\right) f\theta_T' = \varepsilon\left[f'\frac{\partial\theta_T}{\partial\varepsilon} - \theta_T'\frac{\partial f}{\partial\varepsilon} + \frac{B}{R}\left(g'\frac{\partial\theta_T}{\partial\varphi} - \theta_T'\frac{\partial g}{\partial\varphi}\right)\right] \end{aligned}\right\} \quad (16)$$

with

$$\left.\begin{aligned} &f = g = 0, \quad \theta_T = 1 \\ &f' = B^{1/2}\frac{\sin\beta_i \sin\phi}{\sin\varepsilon} \\ &g' = \cos\beta_i + \operatorname{cotg}\varepsilon \sin\beta_i \cos\varphi \end{aligned}\right\} \text{ at } \eta = 0$$
$$f' \to 1, \quad g' \to 0, \quad \theta_T \to 0 \qquad \text{at } \eta \to \infty. \quad (17)$$

In order to use the Görtler type of series [13], we assume that solutions of equations (13) are convergent series of the form [14]

$$\left.\begin{aligned} f(\varepsilon, \eta, \varphi) &= \sum_{N=0}^{\infty} f_N(\eta, \varphi)\varepsilon^N \\ g(\varepsilon, \eta, \varphi) &= \sum_{N=0}^{\infty} g_N(\eta, \varphi)\varepsilon^N \\ \theta_T(\varepsilon, \eta, \varphi) &= \sum_{N=0}^{\infty} \theta_{TN}(\eta, \varphi)\varepsilon^N. \end{aligned}\right\} \quad (18)$$

Upon substituting equations (18) into equations (16) and (17), collecting and equating to zero the coefficient of each power of ε, the following set of differential equations is obtained.

(1) For $N = 0$:

$$\left.\begin{aligned} f_0''' + 2f_0''f_0 - f_0'^2 + Bg_0'^2 + \frac{4}{9}\Omega\theta_{T0} + 1 \\ = g_0'\frac{\partial f_0'}{\partial\phi} - f_0''\frac{\partial g_0}{\partial\varphi} \\ g_0''' + 2(g_0''f_0 - f_0'g_0') = g_0'\frac{\partial g_0'}{\partial\varphi} - g_0''\frac{\partial g_0}{\partial\varphi} \\ Pr^{-1}\theta_{T0}'' + 2f_0\theta_{T0}' = g_0'\frac{\partial\theta_{T0}}{\partial\varphi} - \theta_{T0}'\frac{\partial g_0}{\partial\varphi}. \end{aligned}\right\} \quad (19)$$

It is clear that solutions must not depend on φ at the stagnation point. Thus, all derivatives with respect to φ vanish

$$\left.\begin{aligned} f_0''' + 2f_0''f_0 - f_0'^2 + Bg_0'^2 + \frac{4}{9}\Omega\theta_{T0} + 1 = 0 \\ g_0''' + 2(g_0''f_0 - f_0'g_0') = 0 \\ Pr^{-1}\theta_{T0}'' + 2f_0\theta_{T0}' = 0. \end{aligned}\right\} \quad (20)$$

The boundary conditions are

$$\left.\begin{aligned} f_0 = f_0' = g_0 = 0, \quad \theta_{T0} = 1, \quad g_0' = \cos\beta_i \quad &\text{at } \eta = 0 \\ f_0' \to 1, \quad \theta_{T0} \to 0, \quad g_0' \to 0 \quad &\text{as } \eta \to \infty. \end{aligned}\right\} \quad (21)$$

(2) For $N > 0$ $(N = 1, 2, 3, \ldots)$:

$$f_N''' + B_N^* + \sum_{k=0}^{N}\left[A_k^*\sum_{j=0}^{N-k} f_j f_{N-j-k}'' - B_k^*\sum_{j=0}^{N-k}(f_j'f_{N-j-k}' - g_j'g_{N-j-k}' \cdot B) + \frac{4}{9}\Omega C_k^*\theta_{TN-k}\right]$$
$$= \sum_{k=0}^{N-1}\left[(N-k)(f_k'f_{N-k}' - f_k''f_{N-k}) + BE_k^*\sum_{j=0}^{N-k-1}\left(g_j'\frac{\partial f_{N-j-k}'}{\partial\varphi} - f_j''\frac{\partial g_{N-j-k}}{\partial\varphi}\right)\right]$$

$$g_N''' + \sum_{k=0}^{N}\left[A_k^*\sum_{j=0}^{N-k} g_j'' f_{N-j-k} - 2B_k^*\sum_{j=0}^{N-k} f_j'g_{N-j-k}'\right]$$
$$= \sum_{k=0}^{N-1}\left[(N-k)(f_k'g_{N-k}' - g_k''f_{N-k}) + BE_k^*\sum_{j=0}^{N-k-1}\left(g_j'\frac{\partial g_{N-j-k}'}{\partial\varphi} - g_j''\frac{\partial g_{N-j-k}}{\partial\varphi}\right)\right] \quad (22)$$

$$Pr^{-1}\theta_{TN}'' + \sum_{k=0}^{N} A_k^*\sum_{j=0}^{N-k} f_j\theta_{TN-j-k}'$$
$$= \sum_{k=0}^{N-1}\left[(N-k)(f_k'\theta_{TN-k} - \theta_{Tk}'f_{N-k}) + BE_k^*\sum_{j=0}^{N-k-1}\left(g_j'\frac{\partial\theta_{TN-j-k}}{\partial\varphi} - \theta_{Tj}'\frac{\partial g_{N-j-k}}{\partial\varphi}\right)\right]$$

with

$$\left.\begin{aligned} &f_N = g_N = \theta_{TN} = 0 \\ &f'_N = B^{1/2}F^*_N, \quad g'_N = G^*_N \\ &f'_N \to 0, \quad g'_N \to 0, \quad \theta_{TN} \to 0 \end{aligned}\right\} \quad \begin{aligned} &\text{at } \eta = 0 \\ &\\ &\text{as } \eta \to \infty \end{aligned} \quad \Bigg\} \tag{23}$$

where A^*_k, B^*_k, C^*_k, E^*_k, F^*_k and G^*_N are, respectively, the coefficients of the power series of ε of the following parameters:

$$\left(\frac{1}{2}+\frac{3}{2}\frac{\varepsilon}{R}\frac{\mathrm{d}R}{\mathrm{d}\varepsilon}\right), \quad \frac{\varepsilon}{R}\frac{\mathrm{d}R}{\mathrm{d}\varepsilon}, \quad \frac{\varepsilon \sin\varepsilon}{R^2}, \quad \frac{\varepsilon}{R},$$

$$\frac{\sin\beta_i \sin\varphi}{\sin\varepsilon}, \quad \operatorname{cotg}\varepsilon \sin\beta_i \cos\varphi.$$

Now, in order to reduce equations (20) and (22) into ordinary differential equations, the functions $f_N(\eta,\varphi)$, $g_N(\eta,\varphi)$ and $\theta_{TN}(\eta,\varphi)$ are assumed to have the following expansions:

$$\left.\begin{aligned} f_N(\eta,\varphi) &= \sum_{M=0}^{\infty} f_{N,M}(\eta)\varphi^M \\ g_N(\eta,\varphi) &= \sum_{M=0}^{\infty} g_{N,M}(\eta)\varphi^M \\ \theta_{TN}(\eta,\varphi) &= \sum_{M=0}^{\infty} \theta_{TN,M}(\eta)\varphi^M. \end{aligned}\right\} \tag{24}$$

Series (24) are substituted into equations (20)–(23), using the same procedure as in reducing equations (20)–(23) from equations (16) and (17).

(1) For $N = M = 0$:

$$\left.\begin{aligned} &f'''_{0,0} + 2f''_{0,0}f_{0,0} \\ &\quad -f'^2_{0,0} + Bg'^2_{0,0} + \frac{4}{9}\Omega\theta_{T0,0} + 1 = 0 \\ &g'''_{0,0} + 2(g''_{0,0}f_{0,0} - f'_{0,0}g'_{0,0}) = 0 \\ &Pr^{-1}\theta''_{T0,0} + 2f_{0,0}\theta'_{T0,0} = 0 \end{aligned}\right\} \tag{25}$$

with boundary conditions

$$\left.\begin{aligned} &\eta = 0: \quad f_{0,0} = f'_{0,0} = g_{0,0} = 0, \\ &\qquad\qquad \theta_{T00} = 1, \quad g'_{0,0} = \cos\beta_i \\ &\eta \to \infty: \quad f'_{0,0} \to 1, \quad g'_{0,0} \to 0, \quad \theta_{T0,0} \to 0. \end{aligned}\right\} \tag{26}$$

(2) For $N > 0$ and $M \geqslant 0$:

$$\left.\begin{aligned} &f'''_{N,M} + B^*_N + \sum_{k=0}^{\infty}\Bigg[A^*_k \sum_{j=0}^{N-k}\sum_{l=0}^{M} f_{j,l}f''_{N-j-k,M-l} - B^*_k \sum_{j=0}^{N-k}\sum_{l=0}^{M}(f'_{j,l}f'_{N-j-k,M-l} \\ &\qquad - g'_{j,l}g'_{N-j-l,M-l}\cdot B) + \frac{4}{9}\Omega C^*_k\theta_{TN-k,M}\Bigg] \\ &\quad = \sum_{k=0}^{N-1}\Bigg[(N-k)\sum_{l=0}^{M}(f'_{k,l}f'_{N-k,M-l}) - f''_{k,l}f_{N-k,M-l}) + BE^*_k \sum_{j=0}^{N-k-1}\sum_{l=0}^{M}(M-l+1) \\ &\qquad \times (g'_{j,l}f'_{N-j-k,M-l+1} - f''_{j,l}g_{N-j-k,M-l+1})\Bigg] \\ &g'''_{N,M} + \sum_{k=0}^{N}\Bigg[A^*_k \sum_{j=0}^{N-k}\sum_{l=0}^{M} g''_{j,l}f_{N-j-k,M-l} + 2B^*_k \sum_{j=0}^{N-k}\sum_{l=0}^{M} f'_{j,l}g'_{N-j-k,M-l}\Bigg] \\ &\quad = \sum_{k=0}^{N-1}\Bigg[(N-k)\sum_{l=0}^{M}(f'_{k,l}g'_{N-k,M-l} - g''_{k,l}f_{N-k,M-l}) + BE^*_k \sum_{j=0}^{N-k-1}\sum_{l=0}^{M}(M-l+1) \\ &\qquad \times (g'_{j,l}g'_{N-j-k,M-l+1} - g''_{j,l}g_{N-j-k,M-l})\Bigg] \\ &Pr^{-1}\theta''_{TN,M} + \sum_{k=0}^{N} A^*_k \sum_{j=0}^{N-k}\sum_{l=0}^{M} f_{j,l}\theta'_{TN-j-k,M-l} \\ &\quad = \sum_{k=0}^{N-1}\Bigg[(N-k)\sum_{l=0}^{M}(f'_{k,l}\theta_{TN-k,M-l} - \theta'_{Tk,l}f_{N-k,M-l}) + BE^*_k \sum_{j=0}^{N-k-1}\sum_{l=0}^{M}(M-l+1) \\ &\qquad \times (g'_{j,l}\theta_{TN-j-k,M-l+1} - \theta'_{Tj,l}g_{N-j-k,M-l+1})\Bigg] \end{aligned}\right\} \tag{27}$$

Boundary conditions (23) become

$$\left.\begin{aligned} &f_{N,M} = g_{N,M} = \theta_{TN,M} = 0 \\ &f'_{N,M} = B^{1/2}F^*_{N,M},\ g'_{N,M} = G^*_{N,M} \end{aligned}\right\} \text{at } \eta = 0$$
$$f'_{N,M} \to 0,\ g'_{N,M} \to 0,\ \theta_{TN,M} \to 0 \quad \text{as } \eta \to \infty \qquad (28)$$

where $F^*_{N,M}$ and $G^*_{N,M}$ are the coefficients of the power series of F^*_N and G^*_N in terms of φ. In the foregoing equations, the functions subscribed $(0, l)$ with $l > 0$ are equal to zero. The physical quantities of greatest interest are the local Nusselt number Nu and the components C_ε and C_θ of the local friction factor. These quantities are defined, respectively, by

$$Nu = \frac{hL}{\lambda};\quad C_\varepsilon = \frac{\tau_x}{\frac{1}{2}\rho U_\infty^2};\quad C_\theta = \frac{\tau_\theta}{\frac{1}{2}\rho U_\infty^2} \qquad (29)$$

where τ_x and τ_θ are the components of wall shear stress, ρ is the density and λ is the thermal conductivity of the fluid. With Fourier's law, the heat transfer coefficient h can be expressed as

$$h = \frac{-\lambda\left(\frac{\partial T}{\partial y}\right)_{y=0}}{T_w - T_\infty}. \qquad (30)$$

The definitions of τ_x and τ_θ are

$$\tau_x = \mu\left(\frac{\partial V_x}{\partial y}\right)_{y=0};\quad \tau_\theta = \mu\left(\frac{\partial V_\theta}{\partial y}\right)_{y=0} \qquad (31)$$

where μ is the dynamic viscosity. From equations (29)–(31), it can be shown that

$$Nu\, Re_\infty^{-1/2} = -\left(\frac{3}{2}\frac{\sin\varepsilon}{\varepsilon}\right)^{1/2}\sum_{j=0}^{\infty}\sum_{l=0}^{\infty}\theta'_{Tjl}(0)\varepsilon^j\varphi^l$$
$$\frac{1}{2}C_\varepsilon\, Re_\infty^{1/2} = \left(\frac{3}{2}\sin\varepsilon\right)^{3/2}\varepsilon^{-1/2}\sum_{j=0}^{\infty}\sum_{l=0}^{\infty}f''_{jl}(0)\varepsilon^j\phi^l \qquad (32)$$
$$\frac{1}{2}C_\theta\, Re_\infty^{1/2} = \left(\frac{B}{\varepsilon}\right)^{1/2}\left(\frac{3\sin\varepsilon}{2}\right)^{3/2}\sum_{j=0}^{\infty}\sum_{l=0}^{\infty}g''_{jl}(0)\varepsilon^j\phi^l.$$

The average Nusselt number $\overline{Nu}$ can be obtained from the following integral:

$$\overline{Nu} = \frac{1}{S}\int_{(S)} Nu\, dS \qquad (33)$$

where S is the area of the sphere.

3. RESULTS AND DISCUSSION

Equations (25)–(28) are integrated using the fourth-order Runge–Kutta–Gill procedure. The values of $f''_{N,M}(0)$, $g''_{N,M}(0)$ and $\theta'_{TN,M}(0)$ are determinated with a multiple shooting method [15]. The first five terms of series (18) have been calculated. For $N = 1$ and 2, twelve terms of series (24) are necessary to get accurate results. For $N > 2$, the higher order of φ may be reduced as N increases in order to save computational time. It should be noted that the series in terms of φ are numerically convergent for $-\pi < \varphi < \pi$. The details of the numerical integration are reported in ref. [9] and will not be repeated here.

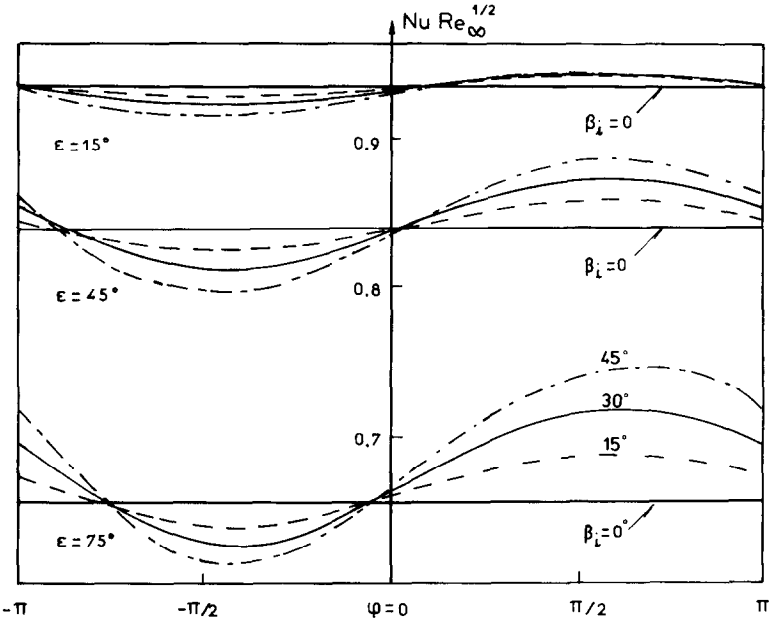

FIG. 2. Angular distributions of the local Nusselt number for $Pr = 1$, $B = 0.5$, $\Omega = 0$: ———, $\beta_i = 15°$; ———, $\beta_i = 30°$; ———, $\beta_i = 45°$.

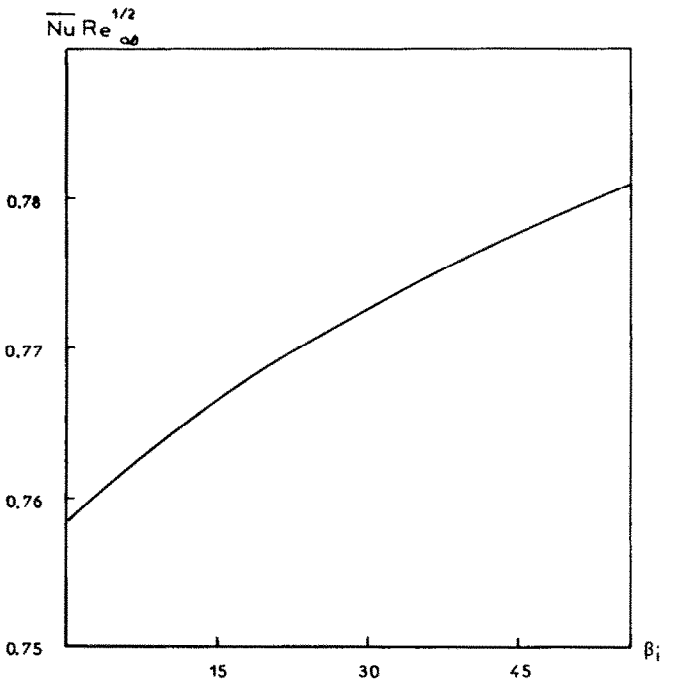

FIG. 3. Average Nusselt number vs β_i. $Pr = 1$, $B = 1$, $\Omega = 0$.

Numerical results were carried out for a Prandtl number of 1 with rotation parameter and buoyancy force parameter values ranging from 0 to 10.

In Fig. 2, distributions of the local Nusselt number $Nu\,Re_\infty^{-1/2}$ at three angular locations ($\varepsilon = 15°$, 45°, 75°) are plotted against φ for $B = 0.5$ and $\Omega = 0$ (pure forced convection) and for several values of β_i. For $\beta_i = 0°$, we observe horizontal lines which indicate that all the points of each angular location ε are subjected to the same flow conditions. These lines are progressively deformed into sinusoidal curves of larger amplitude as β_i increases. Maximal and minimal

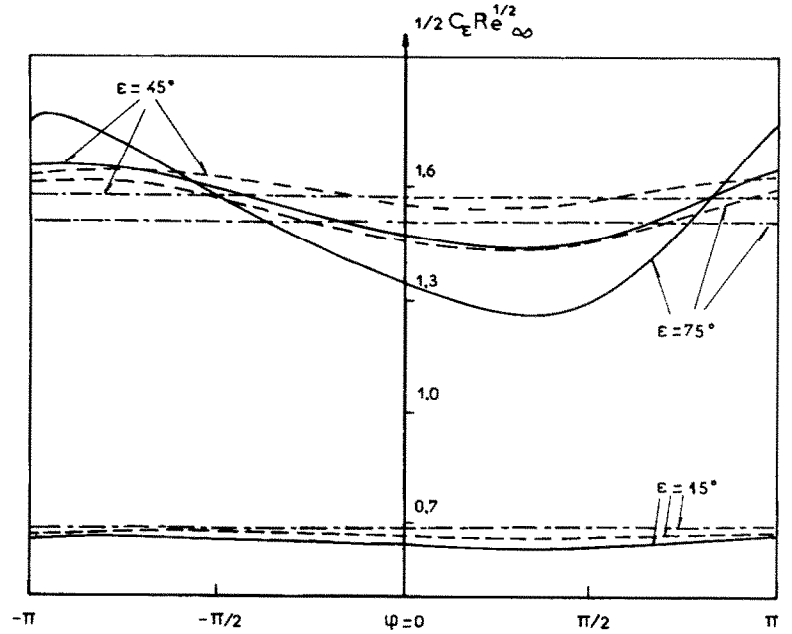

FIG. 4. Angular distributions of the ε component of the local friction factor for $Pr = 1$, $B = 0.5$, $\Omega = 0$: ———, $\beta_i = 0°$; — — —, $\beta_i = 15°$; ———, $\beta_i = 45°$.

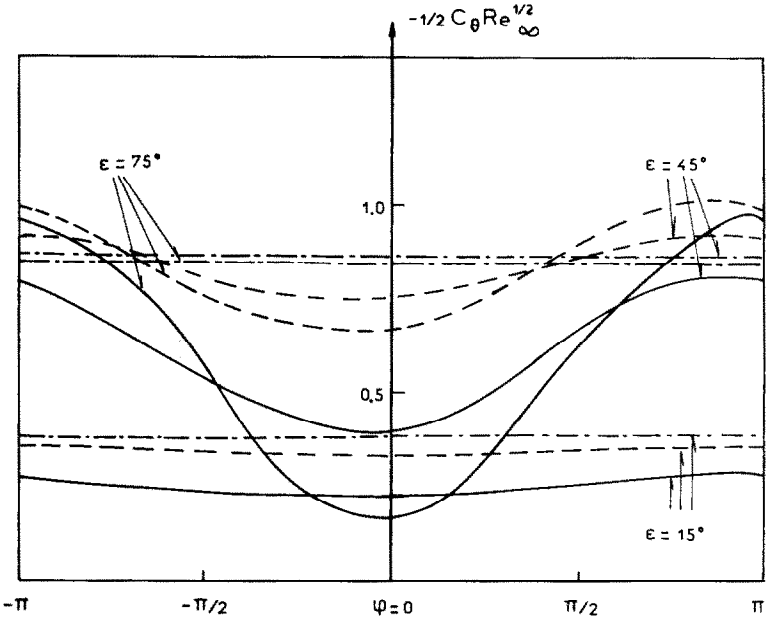

FIG. 5. Angular distributions of the θ component of the local friction factor for $Pr = 1$, $B = 0.5$, $\Omega = 0$: ———, $\beta_i = 0°$; — — —, $\beta_i = 15°$; ———, $\beta_i = 45°$.

values are obtained for $\pi > \varphi > 0$ and $0 > \varphi > -\pi$, respectively, because the centrifugal forces support the forced stream when φ is positive and oppose it when φ is negative. It is interesting to note that the mean value of the Nusselt number, at each ε, is different from that obtained for $\beta_i = 0°$. As a result, the average Nusselt number $\overline{Nu}\, Re_\infty^{-1/2}$ slowly increases with an increasing β_i (Fig. 3), which is in agreement with the experimental investigations of Furuta *et al.* [3].

Figures 4 and 5 show the three-dimensional effects of the flow upon the angular distributions of the axial

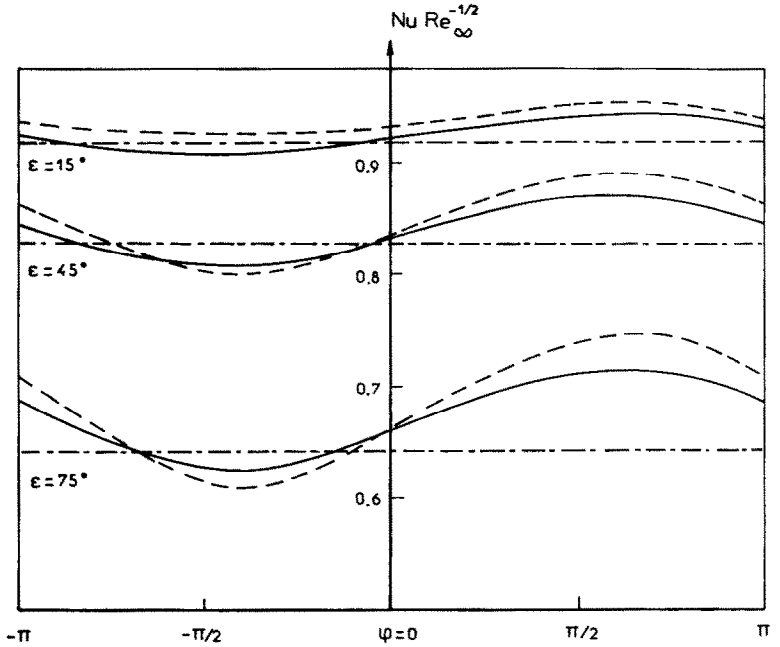

FIG. 6. Angular distributions of the local Nusselt number for several values of the rotation parameter. $Pr = 1$, $\beta_i = 30°$, $\Omega = 0$: — — —, $B = 0$; ———, $B = 0.5$; — — —, $B = 1$.

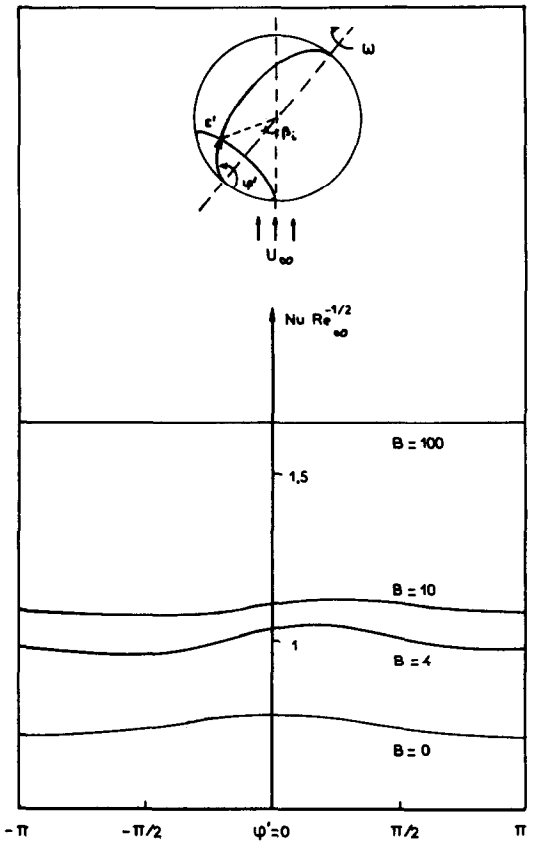

FIG. 7. Angular distributions of the local Nusselt number with respect to the axis of rotation. $\varepsilon' = \beta_i = 15°$, $Pr = 1$, $\Omega = 0$.

and radial components of the local friction factor, expressed as $\frac{1}{2}C_\varepsilon Re_\infty^{1/2}$ and $\frac{1}{2}C_\theta Re_\infty^{1/2}$, respectively. From Fig. 4, it is seen that opposing flow ($\varphi < 0$) produces a larger velocity gradient at the wall with an accompanying increase in the friction factor.

Figure 6 shows the effect of the rotation parameter. The local distributions of the Nusselt number are plotted against φ for $\Omega = 0$, $\beta_i = 30°$ and three values of B (0, 0.5, 1). It is noted that the amplitude of sinusoidal profiles is larger as B increases. Moreover, the local heat transfer rate has a higher value for a higher rotation parameter, which is due to centrifugal effects. It is of interest to compare our results with the experimental ones measured by Furuta *et al.* Unfortunately, the data reported in ref. [3] do not permit a quantitative comparison and so we only study the qualitative effect of B. Figure 7 shows the local Nusselt number profile for $\varepsilon' = \beta_i = 15°$, where ε' is defined in the inset. For $B = 0$ and with respect to the axis of rotation, we get a symmetrical curve with its maximum value at $\varphi' = 0$. This curve is deformed into a sinusoidal shape as B increases, minimum values of the profile occurring in the region $\varphi' < 0$. When the spin velocity ω is high as compared to U_∞, the effect of the oncoming forced stream becomes negligible so that a horizontal straight line is obtained. This change in the shape of the profile as B increases is in qualitative agreement with the result of Furuta *et al.*

The free convective effects on the local heat transfer rate are shown on Fig. 8 where $Nu\,Gr^{-1/4}$ is plotted against φ for $\Omega = 0.5$, 1 and 10, $\beta_i = 30°$ and three angular locations ε. As Ω increases, the deformation

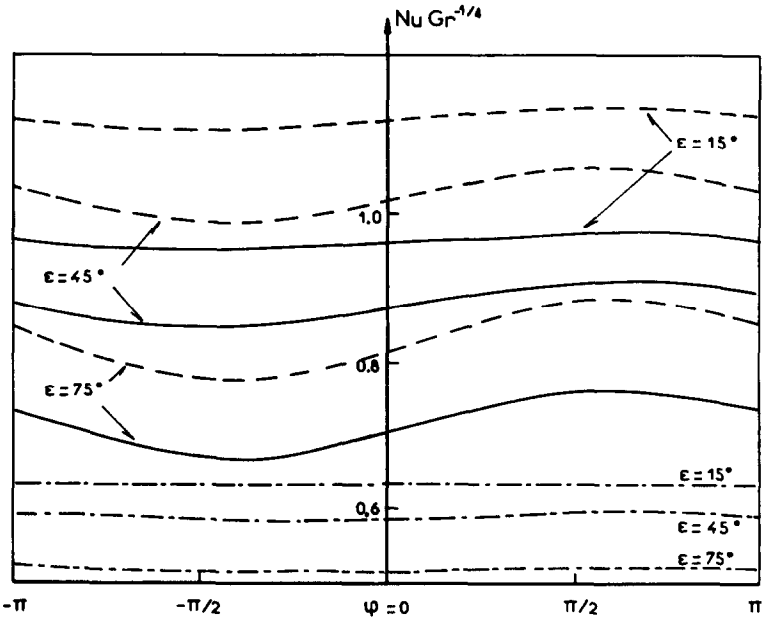

FIG. 8. Angular distributions of the local Nusselt number in terms of $Nu\,Gr^{-1/4}$ for several values of the buoyancy force parameter: $Pr = 1$, $\beta_i = 30°$, $B = 0$: ———, $\Omega = 0.5$; ———, $\Omega = 1$; ———, $\Omega = 10$.

of the profiles is similar to that of the preceding figure. The curves pass from a sinusoidal shape when Ω is low to a horizontal line for $\Omega = 10$, which shows that the heat transfer rate becomes symmetrical with respect to the direction of the forced stream. It is evident that this limiting value of 10 will be higher for a higher value of the rotation parameter.

It should also be noted that our results agree with the theoretical study of Lee *et al.* [1] for the particular case of axial pure forced convection ($\beta_i = \Omega = 0$). These results are compared in Fig. 9 for $B = 1$ and 10.

Before concluding this section, it is of interest to compare the theoretical results with experimental data in order to provide some quantitative comparisons. The average mass transfer coefficient for a rotating sphere in a stream was measured by an electrochemical method. The details of this method have been reported elsewhere [9, 16, 17]. Figure 10 shows the effect of the rotation parameter on the average Sherwood number, $\overline{Sh}$, for $\Omega = 10$ and for several values of β_i (0°, 5°, 10°, 15°). The Schmidt number was equal to 2730 and numerical calculations were performed for this value. As it can be seen, the agreement between the theoretical results and experimental data is satisfactory. However, it may be observed that the theory leads to a larger Sherwood number than the experimental one, specially when B is low. One of the reasons is that the hypothesis of the potential-flow solution provides higher local mass (heat) transfer rates for $60° < \varepsilon < 90°$ [2, 4]: as a result, the average Sherwood (Nusselt) number is greater. The slight discrepancy between the theory and data also results from separation which is predicted to occur for laminar flow over a stationary sphere at $\varepsilon \simeq 110°$. For a rotating sphere in an axial stream, this angle is reduced and it becomes equal to 90° when $\omega L \gg U_\infty$. However, in this last case, equation (33) gives better results because the flow is symmetrical with respect to the equatorial zone [5, 9]. The theoretical increase of $\overline{Sh}$ with increasing β_i shown in Fig. 10 is too small to be validated by the experimental data, which have estimated errors of $\pm 8\%$.

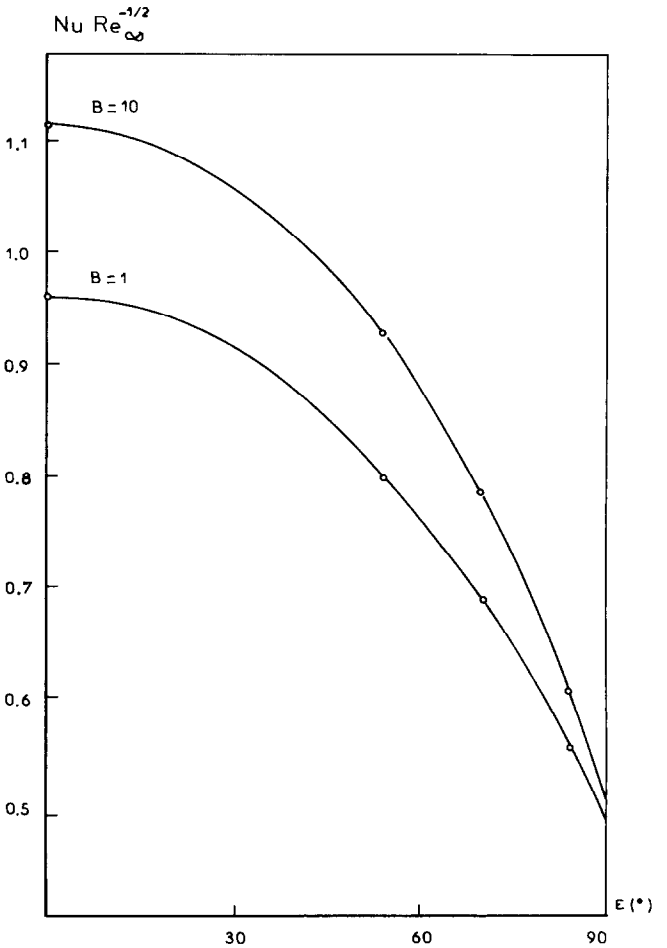

FIG. 9. Comparison of our results with theoretical work of Lee *et al.* [1]. $Pr = 1$, $\beta_i = 0°$, $\Omega = 0$: ———, our results; ○, results of ref. [1].

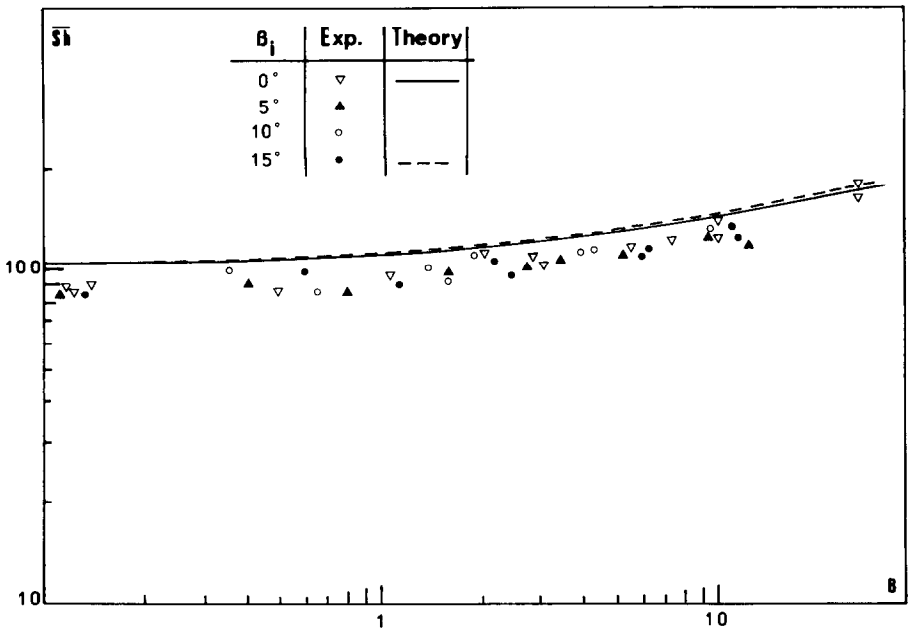

FIG. 10. Effect of the rotation parameter upon the average Sherwood number: comparison between the theory and data [9, 17]. $\Omega = 10$, Schmidt number = 2730.

4. CONCLUSION

The Görtler type of series has been applied to the study of the three-dimensional mixed convection about a rotating sphere which is situated in a forced stream of arbitrary direction with respect to the axis of rotation. Results show the three-dimensional effects of the flow on the local heat transfer rate and the components of the friction factor. The values of the rotation parameter and the buoyancy force parameter range from 0 to 10. For a Prandtl number of 1, our results qualitatively and quantitatively agree with some particular cases reported in the literature. Moreover, experimental investigations by an electrochemical method provide a reasonable agreement between theoretical results and measurements.

REFERENCES

1. M. H. Lee, D. R. Jeng and K. J. De Witt, Laminar boundary layer transfer over rotating bodies in forced flow, *ASME J. Heat Transfer* **100,** 496–502 (1978).
2. T. Furuta, T. Jimbo, M. Okazaki and R. Toei, Mass transfer to a rotating sphere in an axial stream, *J. Chem. Engng Japan* **8,** 456–462 (1975).
3. T. Furuta, M. Okazaki and R. Toei, Mass transfer to a rotating sphere in a stream, *J. Chem. Engng Japan* **10,** 286–292 (1977).
4. T. S. Chen and A. Mucoglu, Analysis of mixed forced and free convection about a sphere, *Int. J. Heat Mass Transfer* **20,** 867 875 (1977).
5. R. K. Bachrun, Etude des couches limites newtoniennes et ostwaldiennes engendrées par la rotation de corps à symétrie de révolution. Application au contrôle hydrodynamique des couches limite de diffusion, Thesis, Perpignan, France (1981).
6. A. Suwono, Buoyancy effects on flow and heat transfer on rotating axisymmetric round-nosed bodies, *Int. J. Heat Mass Transfer* **23,** 819–831 (1980).
7. G. Le Palec and M. Daguenet, Analysis of free convective effects about a rotating sphere in forced flow, *Int. Commun. Heat Mass Transfer* **11,** 409–416 (1984).
8. R. Rajasekaran and M. G. Palekar, Mixed convection about a rotating sphere, *Int. J. Heat Mass Transfer* **28,** 959–968 (1985).
9. G. Le Palec, Etude de la convection mixte tridimensionnelle autour d'une sphère en rotation dans un écoulement ascendant de fluide newtonien, Thesis, Perpignan, France (1986).
10. F. Ayres, *Theory and Problems of Plane and Spherical Trigonometry*. McGraw-Hill, New York (1954).
11. H. Schlichting, *Boundary-layer Theory*, 6th Edn. McGraw-Hill, New York (1968).
12. N. Frossling, Evaporation, heat transfer and velocity distribution in two-dimensional and rotationally symmetrical laminar boundary-layer flow, National Advisory Committee for Aeronautics, TM 1432 (1958).
13. H. Görtler, A new series for the boundary-layer, *J. Math. Mech.* **16,** 1–66 (1957).
14. A. Suwono, Laminar free convection boundary-layer in three-dimensional systems, *Int. J. Heat Mass Transfer* **23,** 53–61 (1981).
15. B. Carnahan, H. A. Luther and J. O. Wilkes, *Applied Numerical Methods*. Wiley, New York (1969).
16. T. Mizushina, *Advances in Heat Transfer*, Vol. 7, p. 87. Academic Press, New York (1971).
17. M. T. Razafiarimanana, G. Le Palec, F. Coeuret et M. Daguenet, Transfert de matière en convection mixte entre une sphère en rotation et un liquide newtonien en écoulement vertical ascendant, *Electrochim. Acta* (1987), in press.

APPENDIX

This section gives the appropriate transformations in order to study the rotation dominated case ($B > 1$, $B > \Omega$) and the buoyancy force dominated case ($\Omega > 1$, $B < \Omega$).

Table A1 summarizes the definitions of the dimensionless coordinates ε, η and φ with the corresponding dimensionless stream functions $f(\varepsilon, \eta, \varphi)$ and $g(\varepsilon, \eta, \varphi)$. For both cases, the dimensionless temperature $\theta_T(\varepsilon, \eta, \varphi)$ is defined by equation (13).

Introducing these transformations in equations (1)–(5) gives the following differential system:

$$f''' + K_1 f'^2 + K_2 g'^2 + K_3 f f'' + K_4 + K_5 \theta_T = \varepsilon\left[f'\frac{\partial f'}{\partial \varepsilon} - f''\frac{\partial f}{\partial \varepsilon} + \frac{1}{R}\left(g'\frac{\partial f'}{\partial \varphi} - f''\frac{\partial g}{\partial \varphi}\right)\right]$$

$$g''' + K_3 g'' f + K_6 g' f' = \varepsilon\left[f'\frac{\partial g'}{\partial \varepsilon} - g''\frac{\partial f}{\partial \varepsilon} + \frac{1}{R}\left(g'\frac{\partial g'}{\partial \varphi} - g''\frac{\partial g}{\partial \varphi}\right)\right]$$

$$Pr^{-1}\theta_T'' + K_3 \theta_T' f = \varepsilon\left[f'\frac{\partial \theta_T}{\partial \varepsilon} - \theta_T'\frac{\partial f}{\partial \varepsilon} + \frac{1}{R}\left(g'\frac{\partial \theta_T}{\partial \varphi} - \theta_T'\frac{\partial g}{\partial \varphi}\right)\right]$$

with

$$f = g = 0;\ \theta_T = 1;\ f' = K_7;\ g' = K_8 \text{ at } \eta = 0 \qquad (34)$$
$$g' \to 0;\ \theta_T \to 0;\ f' \to K_9 \text{ as } \eta \to \infty$$

where the coefficients $K_1, K_2, \ldots$ are given in Table A2.

Equations (34) are treated as explained in Section 2 by introducing successively series (18) and (24).

Table A1. Definition of ε, η, φ, $f(\varepsilon, \eta, \varphi)$ and $g(\varepsilon, \eta, \varphi)$ for the study of the rotation dominated case and the buoyancy force dominated case

	ε	η	φ	$f(\varepsilon, \eta, \varphi)$	$g(\varepsilon, \eta, \varphi)$
Rotation dominated case	$\frac{x}{L}$	$\left(\frac{\omega R}{\nu\varepsilon}\right)^{1/2} y$	θ	$\sqrt{\left(\frac{\omega R}{\nu\varepsilon}\right)}\frac{\psi(x,y,\theta)}{\omega r}$	$\sqrt{\left(\frac{\omega R}{\nu\varepsilon}\right)}\frac{\phi(x,y,\theta)}{\omega r}$
Buoyancy force dominated case	$\frac{x}{L}$	$Gr^{1/4}\frac{y}{L}$	θ	$\frac{\psi(x,y,\theta)}{\varepsilon\nu\, Gr^{1/4}}$	$\frac{\phi(x,y,\theta)}{\varepsilon\nu\, Gr^{1/4}}$

Table A2. Definition of the coefficients of equations (34)

	Rotation dominated case	Buoyancy force dominated case
K_1	$-\frac{\varepsilon}{R}\frac{dR}{d\varepsilon}$	-1
K_2	$\frac{\varepsilon}{R}\frac{dR}{d\varepsilon}$	$\frac{\varepsilon}{R}\frac{dR}{d\varepsilon}$
K_3	$\frac{1}{2} + \frac{3}{2}\frac{\varepsilon}{R}\frac{dR}{d\varepsilon}$	$1 + \frac{\varepsilon}{R}\frac{dR}{d\varepsilon}$
K_4	$\frac{\varepsilon}{R^2} U \frac{dU}{d\varepsilon}(\omega L)^{-2}$	$\frac{1}{\varepsilon}\frac{U}{U_\infty^2}\frac{dU}{d\varepsilon}\Omega^{-1}$
K_5	$\frac{\sin\varepsilon}{R^2}\varepsilon\frac{Gr}{Re_\omega^2}$, $Re_\omega = \frac{\omega L^2}{\nu}$	$\frac{\sin\varepsilon}{\varepsilon}$
K_6	$-\frac{2\varepsilon}{R}\frac{dR}{d\varepsilon}$	$-\left(1 + \frac{\varepsilon}{R}\frac{dR}{d\varepsilon}\right)$
K_7	$\frac{\sin\beta_i \sin\varphi}{\sin\varepsilon}$	$\frac{3}{2\varepsilon}\left(\frac{B}{\Omega}\right)^{1/2}\sin\beta_i \sin\varphi$
K_8	$\cos\beta_i + \operatorname{cotg}\varepsilon \sin\beta_i \sin\varphi$	$\frac{3}{2\varepsilon}\left(\frac{B}{\Omega}\right)^{1/2}(\cos\beta_i \sin\varepsilon + \sin\beta_i \cos\varphi \cos\varepsilon)$
K_9	$B^{-1/2}$	$\frac{3}{2}\Omega^{-1/2}\frac{\sin\varepsilon}{\varepsilon}$

CONVECTION MIXTE TRIDIMENSIONNELLE AUTOUR D'UNE SPHERE EN ROTATION DANS UN ECOULEMENT FORCE

Résumé—On utilise des séries en puissance de plusieurs variables adimensionnelles pour étudier la convection mixte tridimensionnelle autour d'une sphère en rotation placée dans un écoulement forcé dont la direction diffère de celle de l'axe de rotation. Les équations de la couche limite sont intégrées numériquement et les résultats présentés ont été obtenus pour des valeurs modérées du paramètre de rotation et du paramètre de convection naturelle, ces derniers variant entre 0 et 10. Les résultats relatifs à quelques cas particuliers étudiés dans la littérature montrent un bon accord qualitatif. Par ailleurs, la comparaison entre les résultats théoriques et expérimentaux s'avère satisfaisante.

LAMINARE DREIDIMENSIONALE MISCH-KONVEKTION UM EINE ANGESTRÖMTE ROTIERENDE KUGEL

Zusammenfassung—Zum Studium der laminaren Misch-Konvektion um eine willkürlich angeströmte, isotherme, rotierende Kugel wurde eine Potenzreihenentwicklung für verschiedene Variablen aufgestellt, wobei ein 3-dimensionales Geschwindigkeitsfeld vorliegt. Die Grenzschichtgleichungen wurden numerisch gelöst, die Ergebnisse werden für Rotationsparameter und Auftriebsparameter im Bereich von 0 bis 10 dargestellt. Für einige Spezialfälle ergibt sich eine qualitative und quantitative Übereinstimmung mit Literaturangaben. Darüberhinaus ist die Übereinstimmung zwischen den theoretischen und experimentellen Ergebnissen befriedigend.

ЛАМИНАРНАЯ ТРЕХМЕРНАЯ СМЕШАННАЯ КОНВЕКЦИЯ ОКОЛО ВРАЩАЮЩЕЙСЯ СФЕРЫ

Аннотация—Используются степенные ряды нескольких переменных для исследования ламинарной смешанной конвекции около изотермической вращающейся сферы, обтекаемой потоком произвольного по отношению к оси вращения направления, что обуславливает трехмерное распределение скорости. Уравнения пограничного слоя решаются численно. Представлены результаты расчетов для значений параметра, характеризующего вращение, а также параметра, характеризующего подъемные силы в диапазоне от 0 до 10. Для некоторых частных случаев проведено качественное и количественное сравнение с результатами предыдущих работ и показано их хорошее соответствие. Кроме того, получено удовлетворительное совпадение теоретических и экспериментальных результатов.